



# *In situ* immobilization of nickel(II) phthalocyanine on mesoporous SiO<sub>2</sub>/C carbon ceramic matrices prepared by the sol–gel method: Use in the simultaneous voltammetric determination of ascorbic acid and dopamine

Sergio B.A. Barros<sup>a</sup>, Abdur Rahim<sup>a</sup>, Auro A. Tanaka<sup>b,c</sup>, Leliz T. Arenas<sup>d</sup>, Richard Landers<sup>e</sup>, Yoshitaka Gushikem<sup>a,c,\*</sup>

<sup>a</sup> Department of Inorganic Chemistry, Institute of Chemistry, State University of Campinas – UNICAMP, Campinas, SP, Brazil

<sup>b</sup> Department of Chemistry, Technology Center, Federal University of Maranhao – UFMA, Sao Luis, MA, Brazil

<sup>c</sup> National Institute of Science and Technology for Bioanalytics, State University of Campinas – UNICAMP, Campinas, SP, Brazil

<sup>d</sup> Institute of Chemistry, Federal University of Rio Grande do Sul – UFRGS, Porto Alegre, RS, Brazil

<sup>e</sup> Institute of Physics Gleb Wataghin, State University of Campinas – UNICAMP, Campinas, SP, Brazil

## ARTICLE INFO

### Article history:

Received 23 May 2012

Received in revised form 4 September 2012

Accepted 7 September 2012

Available online xxx

### Keywords:

Carbon ceramic materials

Nickel phthalocyanine

Dopamine

Ascorbic acid

Sol–gel

## ABSTRACT

Three carbon ceramic materials with different porosities were prepared by the sol–gel method, using HNO<sub>3</sub>, HF, and HNO<sub>3</sub>/HF as catalysts and the surface areas ( $S_{\text{BET}}$ ) of the products were determined as 246, 201, and 356 m<sup>2</sup> g<sup>-1</sup>, respectively. The materials were characterized using N<sub>2</sub> sorption isotherms, scanning electron microscopy, and conductivity measurements. The matrices were used as supports for the *in situ* immobilization of Ni(II) phthalocyanine (NiPc) on their surfaces. XPS was used to determine the Ni/Si atomic ratios of the NiPc-modified materials. Pressed disk electrodes were prepared with the NiPc-modified matrices, and tested as sensors for dopamine. The electrode prepared using nitric acid showed excellent catalytic activity for the simultaneous determination of ascorbic acid (AA) and dopamine (DA), with sensitivities of 53.02 and 104.17  $\mu\text{A mmol dm}^{-3}$ , respectively. Good repeatability was achieved, with R.S.D. values of 3.67% (AA) and 3.53% (DA), as well as high stability.

© 2012 Elsevier Ltd. All rights reserved.

## 1. Introduction

The construction of electrodes based on porous silica, prepared using the sol–gel method, is of considerable interest due to the potential applications of these devices in the field of electrochemical sensors [1,2]. Carbon ceramic electrodes (CCEs) have received particular attention [3,4], since the combination of the flexibility of the sol–gel process (which enables control of the porosity and surface area of the oxide) with the conducting properties of the carbon materials gives CCEs advantages over other types of carbon-based electrodes. It is possible to obtain a renewable electrode surface, similar to that of carbon paste electrodes (CPEs) [5], that is more robust and possesses high chemical, thermal, and mechanical stability. As the CCEs are based on matrix with controlled porosity, the electrodes prepared using this substrate present good repeatability, when used as an electrochemical sensor [6].

It is well known that the porosity of the silica matrix prepared by the sol–gel method can be controlled using different catalysts. The acid catalysts (such as HNO<sub>3</sub> or HCl) provide a slow kinetics of condensation of the silica precursor (such as TEOS), which results in the formation of microporous silica. On the other hand, a fast kinetics condensation is obtained using HF as catalyst, which reduces the gelation time, and produces mesoporous silica [7,8]. Control of porosity is of fundamental importance in CCEs, because it affects the degree of dispersion and the connectivity of the carbon particles within the silica matrix. In addition, the porosity of the carbon ceramic matrix is an important factor in the modification of the materials by incorporation of electroactive species, such as metallophthalocyanines, in the silica network.

Metallophthalocyanines (MPcs, M = transition metal) are a family of medium sized organic molecules that have broad applications in fields including non-linear optics, molecular electronics, and fabrication of electrochemical sensors [9]. The utility of these complex molecules derives from their attractive properties, including high chemical, thermal, and mechanical stability [10–12]. Moreover, the MPcs can act as catalysts in a variety of electrochemical reactions [12] commonly used to detect analytes such as dissolved oxygen [13], nitric oxide [14,15], cysteine [16], nitrite [17,18], oxalic acid [19,20], ascorbic acid [21], and dopamine [22].

\* Corresponding author at: Department of Inorganic Chemistry, Institute of Chemistry, State University of Campinas – UNICAMP, Campinas, SP, Brazil.  
Tel.: +55 19 3521 3053; fax: +55 19 3521 3023.

E-mail address: [gushikem@iqm.unicamp.br](mailto:gushikem@iqm.unicamp.br) (Y. Gushikem).

Dopamine (3,4-dihydroxyphenyl ethylamine, DA) is an important neurotransmitter in the central nervous system of mammals. An excess or deficiency of DA can result in brain disorders such as schizophrenia and Parkinson's disease [23,24], as a result of which there is a need for techniques able to detect DA in biological samples. Electrochemical determination of DA by direct oxidation using the commonly employed electrodes is difficult, mainly due to co-oxidation of ascorbic acid (AA) at a potential similar to that of DA. Many efforts have been made to tackle the problem, using a variety of modified electrodes [25–27].

In the present work, three different types of carbon ceramic material were prepared, employing  $\text{HNO}_3$ , HF, or  $\text{HNO}_3/\text{HF}$  as the catalyst in a two-step sol–gel process. The morphology, pore structure, and mechanical properties of the materials were evaluated. Nickel(II) phthalocyanine (NiPc) was synthesized *in situ* in the pores of the carbon ceramic matrices. The materials obtained ( $\text{SiO}_2/\text{C}/\text{NiPc}$ ) were employed to fabricate rigid disk electrodes, which were used for the voltammetric determination of DA. The electrode obtained using  $\text{HNO}_3$  as catalyst was also used for the simultaneous determination of DA and AA.

## 2. Experimental

### 2.1. Reagents

All the reagents used in this work were of analytical grade: tetraethyl orthosilicate, TEOS (Acros, 98%), HF (Vetec, 48%), graphitic carbon (Aldrich, 99.99%,  $S_{\text{BET}} = 9 \text{ m}^2 \text{ g}^{-1}$ ),  $\text{HNO}_3$  (Nuclear, 70%), nickel(II) acetate tetrahydrate (Sigma), phthalonitrile (Fluka, 98%), dopamine (Sigma), ascorbic acid (Merck), KCl (Vetec, 99%), ethanol (Synth, 99.9%); KOH (Synth), physiological solution (Arboeto) and HCl (37%, Synth).

### 2.2. Preparation of the $\text{SiO}_2/\text{C}$ –graphite matrices by the sol–gel method

The  $\text{SiO}_2/\text{C}$ –graphite matrices (SG) were prepared in a two-step sol–gel process, using TEOS and the three different catalysts: (i)  $\text{HNO}_3$ , (ii) HF, and (iii) a mixture of  $\text{HNO}_3$  and HF, added during different steps of the synthesis. The matrices obtained were designated as SGN, SGF, and SGNF, respectively. A 1:1 (w/w)  $\text{SiO}_2/\text{C}$ –graphite ratio was used for the preparation of all three carbon ceramic materials. The SGN matrix was prepared in two steps. The first step involved prehydrolysis by adding 4.8 mL of an aqueous solution of  $3.48 \text{ mol dm}^{-3}$   $\text{HNO}_3$  to 50 mL of a 1:1 (v/v) solution of TEOS and absolute ethanol. The resulting solution was stirred continuously under reflux for 3 h. In the second step, the solution was cooled to room temperature, and 4.0 mL of deionized water, together with a quantity of C–graphite calculated from the expected  $\text{SiO}_2$  weight, was then added under continuous stirring. This mixture was sonicated until gelation of the material occurred, after approximately 2 h. For the SGF matrix, only 4.0 mL of deionized water was added to the TEOS/ethanol mixture in the prehydrolysis step, followed by addition of 4.0 mL of deionized water and 0.5 mL of HF (48%) in the final step. The reaction conditions (duration, temperature, and stirring) were the same as those used for the preparation of SGN. The SGNF matrix was prepared by adding  $\text{HNO}_3$  in the prehydrolysis step, followed by HF addition using the same quantities and conditions described for SGN and SGF. For SGF and SGNF, the time required for gelation under sonication was about 20 min.

The materials obtained (SGN, SGF, and SGNF) were stored under an extraction hood at room temperature for about one week, until solvent evaporation was complete. The resultant xerogel powders were immersed separately in 60 mL of  $2.0 \text{ mmol dm}^{-3}$  HCl,

stirred for 40 min, then filtered and washed with deionized water. The materials were subsequently thoroughly washed with absolute ethanol for 3 h in a Soxhlet extractor, and then dried at 393 K under dynamic vacuum ( $\sim 0.15 \text{ Pa}$  pressure) to completely remove the solvent.

### 2.3. *In situ* synthesis of Ni(II) phthalocyanine in the pores of the $\text{SiO}_2/\text{C}$ –graphite matrices

NiPc was synthesized *in situ* in the pores of the carbon ceramics matrices, as described elsewhere for a similar material [28]. Briefly, 1.0 g of  $\text{SiO}_2/\text{C}$ –graphite was immersed in 10 mL of  $0.02 \text{ mol dm}^{-3}$  nickel(II) acetate tetrahydrate ( $\text{Ni}(\text{OAc})_2 \cdot 4\text{H}_2\text{O}$ ), with continuous stirring for 30 min, followed by heating of the mixture in a glycerin bath at 343 K until the solvent had completely evaporated.

The dry solid (designated  $\text{SiO}_2/\text{C}/\text{Ni}(\text{II})$ ) was weighed out, mixed with an equal amount of phthalonitrile, and heated in an ampoule at 473 K for 3 h to form the NiPc complex. The nickel(II) phthalocyanine not confined in the matrix pores, together with any unreacted phthalonitrile, was removed from the solid surface by washing with absolute ethanol in a Soxhlet extractor. The solid was then heated at 383 K under dynamic vacuum ( $\sim 0.15 \text{ Pa}$  pressure) to evaporate all the solvent. The  $\text{SiO}_2/\text{C}/\text{NiPc}$  materials obtained in this synthesis were designated as SGN/NiPc, SGF/NiPc, and SGNF/NiPc, depending on the carbon ceramic matrix used.

### 2.4. Apparatus

$\text{N}_2$  adsorption–desorption isotherms for the three carbon ceramic materials (SGN, SGF, and SGNF), which had been previously degassed at 423 K, were obtained at the liquid nitrogen boiling point using an Autosorb automated gas sorption analyzer (Quantachrome Instruments, USA). The specific surface area was obtained by the BET (Brunauer, Emmett, and Teller) multipoint method [29]. The pore size distribution was obtained using the BJH (Barret, Joyner, and Halenda) method [30].

Scanning electron microscopy (SEM) images were recorded with a JEOL JSM 6360LV microscope, operated at 20 kV and connected to a secondary back-scattered electrons detector, with energy dispersive X-ray spectroscopy (EDS) for elemental mapping. The samples ( $\sim 1 \text{ mg}$ ) were dispersed onto double-faced conducting tape (3M Electrical Division, Brazil), on an aluminum support, and coated with a gold layer using a Bal-Tec MD20 metallizing system.

The electrical conductivities ( $\sigma$ ) were calculated using 0.5 cm diameter disks, produced by pressing each finely powdered  $\text{SiO}_2/\text{C}$  matrix under a load of  $1.82 \times 10^7 \text{ Pa}$ . The value of  $\sigma$  was obtained as described previously [31], considering the circular disks to have finite lateral dimensions, and applying the equation  $\sigma = (RwF_2F_4)^{-1}$ , where  $R$  is the electrical resistance,  $w$  is the thickness of the disk (0.01 cm), and  $F_2$  and  $F_4$  are the correction factors taken from the literature (0.50 and 0.98, respectively) [31]. The  $R$  values of the carbon ceramics were obtained at room temperature using the four point probe method, with a National Instruments NI PXI-1033 analyzer.

The electronic spectra of NiPc prepared *in situ* in the three carbon ceramic materials were measured by the diffuse reflectance technique, using a Cary 5G UV/Vis spectrophotometer. Barium sulfate was used as a reference sample. The Kubelka–Munk function was used for the diffuse reflectance spectrum analysis.

X-ray photoelectron spectra (XPS) of the powdered materials, fixed on a steel holder with double-faced adhesive tape, were obtained at a pressure of  $2.6 \times 10^{-5} \text{ Pa}$  using a McPherson ESCA-36 spectrometer. The X-ray source was fitted with an Al K anode (1486.6 eV), operated at 10 kV and 15 mA, with a pass energy of 40 eV. The binding energies were calibrated against the Si 2p level (103.5 eV).

## 2.5. Electrochemical experiments

The rigid disk working electrodes were prepared by subjecting 25 mg of each  $\text{SiO}_2/\text{C}/\text{NiPc}$  material to a load of  $1.82 \times 10^7$  Pa, under normal atmospheric conditions. The resultant disks (diameter 0.5 cm, thickness  $\sim 0.01$  cm, and geometric area  $0.20 \text{ cm}^2$ ) were immersed in pure fused paraffin at 353 K under vacuum ( $\sim 0.15$  Pa), until all adsorbed gas had been completely eliminated from the pores of the matrices. Each disk was then attached (with cyanoacrylate ester glue) to the end of a glass tube that had the same cross-sectional area, and the electrical contact was made using a copper wire inserted inside the glass tube. Pure graphite powder was added to the tube in order to improve the connection between the copper wire and the surface of the disk.

The measurements were performed using a PGSTAT-20 (Autolab) potentiostat–galvanostat, connected to an electrochemical cell containing a working electrode (consisting of the prepared material), a reference electrode (SCE), and a counter electrode (Pt wire). All the measurements were carried out using 25 mL of  $0.5 \text{ mol dm}^{-3}$  KCl supporting electrolyte solution, under a nitrogen atmosphere. The pH of the electrolyte was adjusted by adding solutions of KOH or HCl.

## 3. Results and discussion

### 3.1. Characterization of the $\text{SiO}_2/\text{C}$ –graphite matrices

#### 3.1.1. Micrograph images

Fig. 1 shows SEM images of the xerogel particles composed of the three materials obtained by the sol–gel process, together with EDS mapping images of C for these materials. The SEM images show that the morphology of each  $\text{SiO}_2/\text{C}$  matrix was different (Fig. 1a–c). The SGN matrix, produced using  $\text{HNO}_3$  as the sol–gel catalyst, presented a morphology that was less grainy and rough than the other two materials, indicative of a material that was more compact and less porous. The more granular and rough morphology of the carbon ceramic matrix obtained using HF as catalyst (SGF) was suggestive of a more porous material. The SGNF material, produced using a mixture of  $\text{HNO}_3$  and HF as the catalyst, showed morphology intermediate to those of SGN and SGF.

The EDS images of the xerogel particles composed of the three materials revealed light gray zones corresponding to C particles (Fig. 1a'–c'). The distribution of light gray points indicated that there were no segregated domains of C particles when either HF (Fig. 1c') or the mixture of  $\text{HNO}_3$  and HF (Fig. 1b') were used as catalysts.

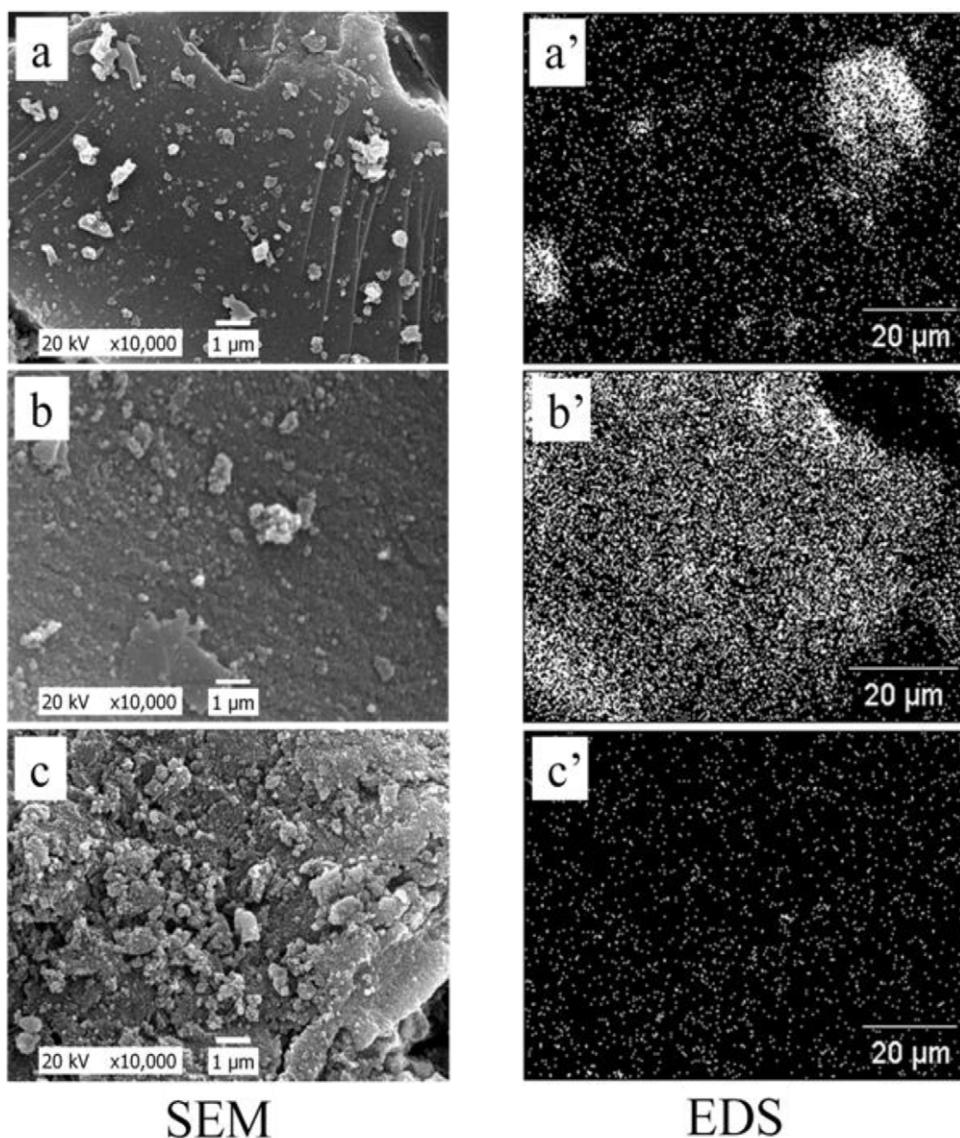
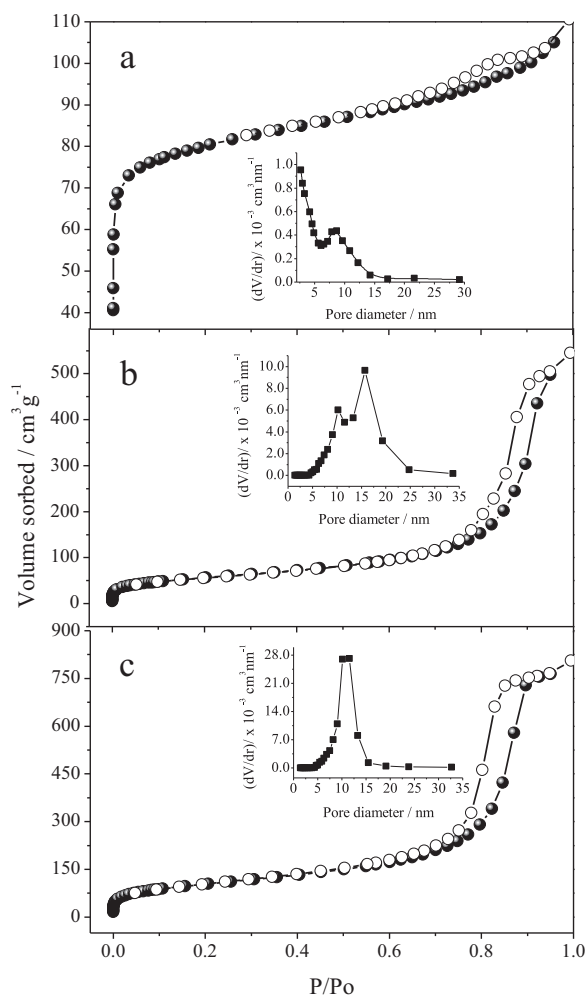


Fig. 1. SEM images for (a) SGN, (b) SGNF, and (c) SGF. EDS images: carbon mapping for (a') SGN, (b') SGNF, and (c') SGF.



**Fig. 2.**  $N_2$  adsorption–desorption isotherms for (a) SGN, (b) SNF, and (c) SGNF, together with the corresponding pore size distribution curves (insets).

This suggests that there were uniform distributions of C particles in the silica networks of SGF and SGNF. There was a comparatively poor dispersion of C particles in the silica network when  $HNO_3$  was used as catalyst (Fig. 1a').

### 3.1.2. Nitrogen adsorption–desorption isotherms

Fig. 2 shows the  $N_2$  adsorption–desorption isotherms of the three carbon ceramic matrices prepared with different catalysts. The  $N_2$  sorption isotherms obtained for the SGF and SGNF matrices suggested a predominance of mesopores, relative to micropores (type IV curve) [32], with a wide pore size distribution in the range 5–25 nm for SGF, and a well defined pore size distribution with a peak at around 11 nm for SGNF (insets to Fig. 2b and c, respectively). In contrast, the  $N_2$  sorption isotherm for SGN was indicative of a predominance of micropores, rather than mesopores (Fig. 2a inset) [33].

The surface areas ( $S_{BET}$ ,  $m^2 g^{-1}$ ) and pore volumes ( $p_v$ ,  $cm^3 g^{-1}$ ) obtained from the isotherms were: (a) SGN,  $S_{BET} = 246$ ,  $p_v = 0.17$ ; (b) SGF,  $S_{BET} = 201$ ,  $p_v = 0.85$ ; and (c) SGNF,  $S_{BET} = 356$ ,  $p_v = 1.20$ . The slight difference between SGN and SGF in the specific surface areas can be explained by the smaller diameter and pore volume displayed by SGN. Both  $S_{BET}$  and  $p_v$  were higher for SGNF, which showed a well defined pore size distribution, and a peak pore diameter that was intermediate to those of SGN and SGF.

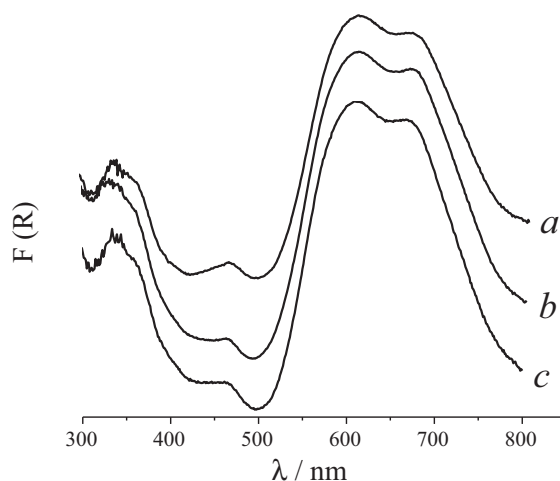


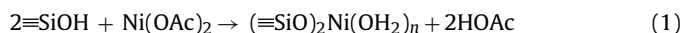
**Fig. 3.** Diffuse reflectance spectra of: (a) SGN–NiPc, (b) SGF–NiPc and (c) SGNF–NiPc.

### 3.1.3. Conductivity

The conductivities obtained for SGN, SGF, and SGNF were 0.88, 0.10, and  $0.03 S cm^{-1}$ , respectively. As Si is more susceptible to nucleophilic attack by the  $F^-$  ion, the electron density in the former atom is reduced, resulting in an increase of the condensation reactions, and consequently a decreased TEOS gelation time [8,34]. At shorter gelation times, a larger amount of graphite carbon can become entrapped in the silica matrix before deposition, which could decrease the percolation of graphitic particles into the silica. The results showed that the materials with smaller pore size and segregated domains of graphite carbon particles presented higher conductivity, due to increased percolation of graphitic particles into the silica network.

### 3.1.4. In situ preparation of NiPc on $SiO_2/C$ matrices

The performance of the carbon ceramic matrices as modified electrodes was investigated after the *in situ* synthesis of NiPc within the pores of the matrices. The *in situ* formation of NiPc can be described in two reaction steps. In the first step, the Ni(II) was attached to the matrix surface through the reaction of nickel acetate with the Brönsted acid groups ( $\equiv SiOH$ ) present on the silica surface, producing the  $SiO_2/C/Ni(II)$  solid (Eq. (1)). The adsorbed Ni(II) acted as a template for phthalocyanine complex formation inside the matrix pores. In the second step, NiPc was formed in the pores of the matrix surface by heating the matrix with adsorbed metal at 473 K in the presence of phthalonitrile (Eq. (2)).



UV–vis diffuse reflectance spectra of the solid materials obtained SGN/NiPc, SGF/NiPc, and SGNF/NiPc (Fig. 3) revealed two broad electronic bands at 612 and 670 nm, assigned as Q bands for Ni(II) under slightly distorted  $D_{4h}$  symmetry as similarly observed for other transition metal phthalocyanine [35]. The Soret or B band could be observed at around 350 nm.

### 3.1.5. X-ray photoelectron spectra

Table 1 summarizes the binding energy (BE) values derived from the X-ray photoelectron spectroscopy analyses for SGN/NiPc, SGF/NiPc, and SGNF/NiPc, together with the Ni/Si atomic ratios. In SGN/NiPc, SGF/NiPc and SGNF/NiPc, the Ni  $2p_{3/2}$  BE was fitted with a curve centered at 854.5 eV and other peaks, centered at 399 and 402 eV with the N 1s BE, assigned to the pyrrolic and meso-nitrogen atoms in NiPc [36]. For SGN/NiPc a second peak centered

**Table 1**  
XPS data for the SGN/NiPc, SGF/NiPc, and SGNF/NiPc materials.

Sample	Binding energy (eV)				Atomic ratio Ni/Si
	Ni 2p <sub>3/2</sub>		N 1s		
SGN/NiPc	854.2	856.6	399.2	403.1	0.04
SGF/NiPc	854.5		398.0	401.9	0.01
SGNF/NiPc	854.5		399.0	402.5	0.01

at 856.6 eV is also observed, assigned to the Ni(OH)<sub>2</sub> at the surface of SiO<sub>2</sub>/C [37,38] formed due to unreacted Ni(II) confined in the pores of the carbon ceramic matrix. Additionally, the Ni/Si atomic ratios obtained by XPS suggested that the amount of NiPc on the surface of the SGN matrix was higher than that on the surfaces of the other two materials.

## 3.2. Electrochemical measurements

### 3.2.1. Electrochemical oxidation of DA on the surface of NiPc-modified CCEs

The importance of differential pulse voltammetry (DPV) in quantitative electrochemical analysis lies in its superior elimination of the background current. The sensitivity and resolution of DPV are much higher than can be achieved using cyclic voltammetry, and the technique was therefore used for the electrochemical measurements in the present study. Fig. 4a shows the DPV results for the carbon ceramic electrodes SGN/NiPc, SGF/NiPc, and SGNF/NiPc, in the presence of  $1.27 \times 10^{-3} \text{ mol dm}^{-3}$  dopamine. Unlike the SGNF/NiPc and SGF/NiPc electrodes, a well-defined narrow oxidation peak was observed for the SGN/NiPc electrode. DPV measurements were recorded for the three NiPc-modified CCEs, using concentrations of DA in the range  $1.00 \times 10^{-4}$  to  $1.27 \times 10^{-3} \text{ mol dm}^{-3}$ . Fig. 4b shows the calibration curves obtained using the three NiPc-modified CCEs for the oxidation of DA at different concentrations.

The SGN/NiPc and SGF/NiPc electrodes provided linear relationships between the peak currents and DA concentrations in the range  $1.00 \times 10^{-4}$  to  $1.27 \times 10^{-3} \text{ mol dm}^{-3}$ . For the SGNF/NiPc electrode, linearity was observed between the peak currents and DA concentrations in the range  $1.00\text{--}8.84 \times 10^{-4} \text{ mol dm}^{-3}$ . The following linear regression equations were obtained:  $\Delta I_{pa} (\mu\text{A}) = 80.32 (\pm 0.78) [\text{DA}] (\text{mmol dm}^{-3}) + 0.13 (\pm 0.60)$ ,  $r = 0.999$

(SGN/NiPc);  $\Delta I_{pa} (\mu\text{A}) = 41.39 (\pm 0.23) [\text{DA}] (\text{mmol dm}^{-3}) - 0.65 (\pm 0.17)$ ,  $r = 0.999$  (SGF/NiPc); and  $\Delta I_{pa} (\mu\text{A}) = 10.58 (\pm 0.16) [\text{DA}] (\text{mmol dm}^{-3}) + 0.22 (\pm 0.09)$ ,  $r = 0.994$  (SGNF/NiPc).

The limit of detection (LOD) was calculated using  $3s_B/S$ , where  $s_B$  is the standard deviation obtained from 10 blank measurements, and  $S$  is the sensitivity of the measurement (slope of the calibration curve) [39].

The limits of detection ( $\mu\text{mol dm}^{-3}$ ) were 0.35, 1.77, and 2.13, for SGN/NiPc, SGF/NiPc, and SGNF/NiPc, respectively.

The SGN/NiPc electrode was more sensitive than the other electrodes investigated for the quantification of DA. This electrode was therefore selected for the electrochemical determination of DA in the presence of AA, and for the simultaneous determination of DA and AA. The greater sensitivity shown by the SGN/NiPc electrode could be explained by the higher conductivity of the SGN material. In addition, the XPS measurements showed that there was a larger quantity of electroactive Ni(II) species present on the surface of the SGN/NiPc electrode. The morphology of the silica matrix is very important, and exerts a major influence on the electrochemical properties of NiPc-modified CCEs.

### 3.2.2. Electrocatalytic oxidation of DA and AA on the SGN/NiPc electrode surface

DPV was used for simultaneous determination of DA in the presence of AA, using the SGN/NiPc electrode. Good peak separation was achieved for the electrooxidation of AA and DA in  $0.5 \text{ mol dm}^{-3}$  KCl solution (pH 5.0) (Fig. 5). The DPV measurement performed using the unmodified SGN electrode showed overlapping low-intensity peaks (dotted line) for the oxidation of AA and DA (Fig. 5a). The broad peaks obtained suggest that the kinetics of electron transfer was slow on the surface of the SGN electrode. However, when the experiment was carried out using the SGN/NiPc electrode (solid line), two well-defined and well-separated high current intensity peaks were obtained for the oxidation of both AA and DA (Fig. 5b). The approximately 250 mV separation of the peak potentials permits the simultaneous determination of AA and DA by cyclic voltammetry. The oxidation of AA and DA on the SGN/NiPc electrode surface can be explained in terms of electrocatalysis, manifested itself in a decrease in the overvoltage and an increase in the oxidation current intensity of the analytes. The results showed that the NiPc adsorbed on the C/SiO<sub>2</sub> surface played a catalytic role in the electrooxidation of these compounds.

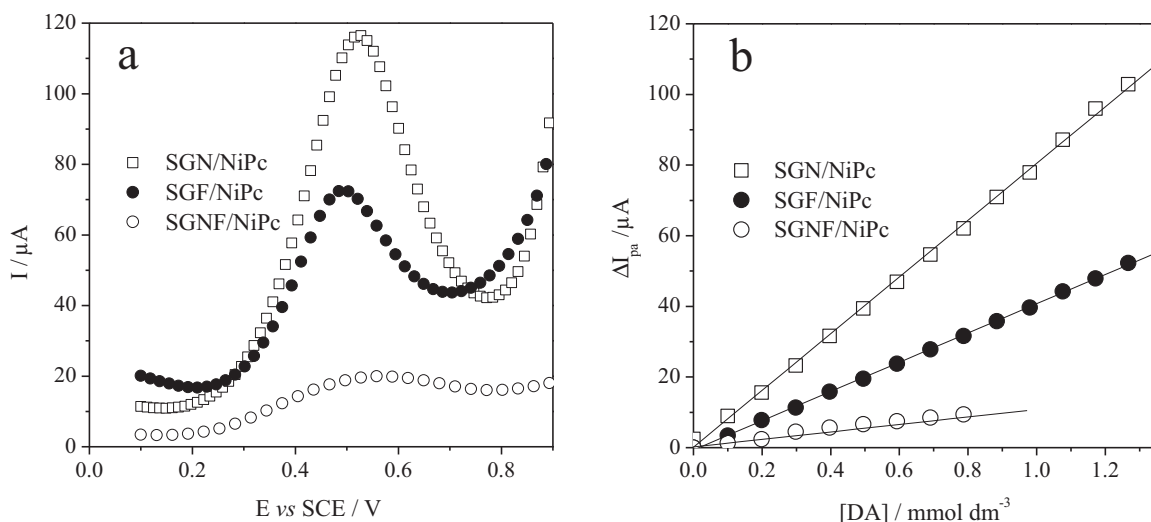


**Fig. 4.** (a) Differential pulse voltammograms recorded for the three NiPc-modified CCEs using  $1.27 \times 10^{-3} \text{ mol dm}^{-3}$  of DA. (b) Calibration curves obtained using the three NiPc-modified CCEs for determination of dopamine at different concentrations.

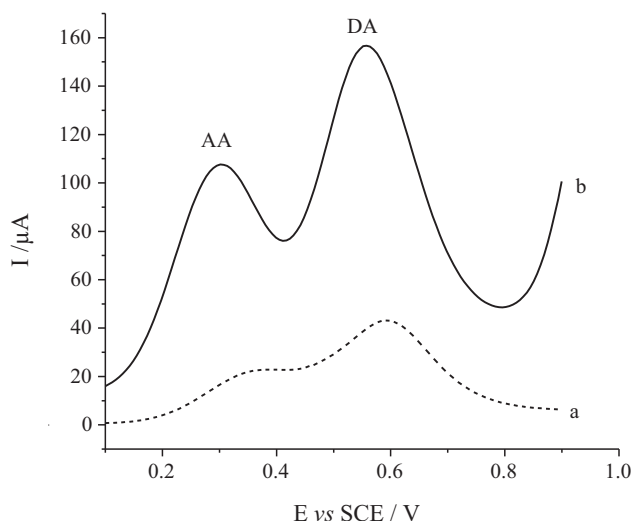


**Fig. 5.** Differential pulse voltammograms of  $1.27 \times 10^{-3} \text{ mol dm}^{-3}$  AA and  $1.27 \times 10^{-3} \text{ mol dm}^{-3}$  DA, in  $0.5 \text{ mol dm}^{-3}$  KCl solution (pH 5.0), using (a) the SGN electrode and (b) the SGN/NiPc electrode.

### 3.2.3. Effect of pH on the electrooxidation of DA and AA on the SGN/NiPc electrode

The effect of pH was investigated in order to optimize the electrocatalytic response of the modified electrode for the oxidation of DA in the presence of AA. The pH of the electrolyte solution had a significant influence on the oxidation potentials of both analytes. DPV measurements were recorded using the SGN/NiPc electrode in  $0.5 \text{ mol dm}^{-3}$  KCl, at pH 2.0–9.0, containing  $9.80 \times 10^{-4}$  and  $5.93 \times 10^{-4} \text{ mol dm}^{-3}$  of AA and DA, respectively. At higher pH, there was a shift of the peak potentials of DA ( $pK_a = 8.87$ ) toward more negative values, due to increased deprotonation during the oxidation process. A decrease in peak potentials for AA was observed between pH 2.0 and pH 4.0, followed by a slight increase at  $pH \geq 5.0$ . AA ( $pK_a 4.17$ ) exists in a neutral form in solutions with  $pH \leq 4.0$ , and in an anionic form in solutions with  $pH \geq 5.0$ , which could result in repulsive electrostatic interactions on the modified electrode surface, since the isoelectric point of silica lies between pH 2.0 and pH 3.0 [40]. The maximum anodic peak currents for AA were obtained at  $pH \sim 5.0$ , whereas the peak current values for DA oxidation showed maxima at lower pH, with a plateau between pH 4.0 and pH 6.0, followed by a progressive decrease at  $pH \geq 6.0$ . Maximum separation of the AA and DA peak potentials was obtained at pH 5.0. This pH value was therefore selected in all subsequent experiments in order to maximize selectivity and sensitivity.

### 3.2.4. Effect of scan rate on the electrooxidation of DA and AA on the SGN/NiPc electrode

The influence of scan rate ( $\nu$ ) was evaluated by recording cyclic voltammograms using the SGN/NiPc electrode with  $1.27 \times 10^{-3} \text{ mol dm}^{-3}$  AA and  $1.27 \times 10^{-3} \text{ mol dm}^{-3}$  DA, at different scan rates in the range  $5\text{--}100 \text{ mV s}^{-1}$ . For both analytes, a linear relationship was found between the anodic peak current and the square root of the scan rate, indicative of a diffusion-controlled electrode process. This type of behavior is suitable for quantitative applications. The following linear regression equations were obtained:  $I_{pa} (\mu\text{A}) = 2.32 (\pm 0.85) + 8.36 (\pm 0.12) \nu^{1/2} (\text{V s}^{-1})^{1/2}$ ,  $r = 0.999$  (AA);  $I_{pa} (\mu\text{A}) = 4.74 (\pm 1.31) + 11.86 (\pm 0.19) \nu^{1/2} (\text{V s}^{-1})^{1/2}$ ,  $r = 0.999$  (DA). Linear relationships were also found between the logarithms of the peak currents and the logarithms of the scan rates, with slopes of 0.46 and 0.43 for AA and DA, respectively. These values are in close agreement with the theoretical value of 0.5 expected for an ideal reaction involving solution species and

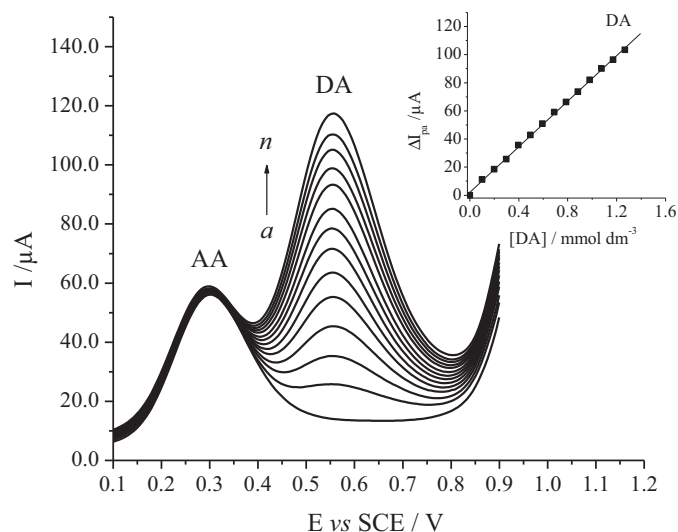


**Fig. 6.** Differential pulse voltammograms of DA in the presence of  $0.7 \text{ mmol dm}^{-3}$  AA, recorded using the SGN/NiPc electrode in  $0.5 \text{ mol dm}^{-3}$  KCl solution (pH 5.0). DA concentrations (from a to n):  $1.00 \times 10^{-4}$ ,  $2.00 \times 10^{-4}$ ,  $2.98 \times 10^{-4}$ ,  $3.97 \times 10^{-4}$ ,  $4.95 \times 10^{-4}$ ,  $5.93 \times 10^{-4}$ ,  $6.90 \times 10^{-4}$ ,  $7.87 \times 10^{-4}$ ,  $8.84 \times 10^{-4}$ ,  $9.80 \times 10^{-4}$ ,  $1.08 \times 10^{-3}$ ,  $1.17 \times 10^{-3}$ , and  $1.27 \times 10^{-3} \text{ mol dm}^{-3}$ . The inset shows the calibration curve for DA.

a purely diffusion-controlled current. In addition, plots of the peak currents normalized to the scan rate ( $I_{pa}/\nu^{1/2}$ ), against the scan rate, exhibited shapes characteristic of an  $\text{EC}_{\text{cat}}$  process [41,42].

### 3.2.5. Identification of DA in the presence of AA on the SGN/NiPc electrode surface

AA is the main interferent in electroanalytical determinations of DA. The influence of increased concentrations of DA in the presence of  $0.7 \text{ mmol dm}^{-3}$  AA was studied using the SGN/NiPc electrode (Fig. 6). In these measurements, only the concentration of DA was varied, while the concentration of AA remained fixed. As shown in Fig. 6, the electrochemical response of DA increased linearly with concentration. However, changes in DA concentration did not have any significant influence on the current intensity and peak potential of AA.

The calibration curve for DA in the presence of AA is shown in the inset of Fig. 6. Within the concentration range  $1.00 \times 10^{-4}$  to  $1.27 \times 10^{-3} \text{ mol dm}^{-3}$ , the following linear regression equation was obtained for the curve:  $\Delta I_{pa} (\mu\text{A}) = 81.16 (\pm 0.78) [\text{DA}] (\text{mmol dm}^{-3}) + 2.09 (\pm 0.60)$ ,  $r = 0.999$ . The limit of detection calculated for DA was  $0.34 \mu\text{mol dm}^{-3}$ . This has a lower limit of detection than that obtained for measurement of DA in the presence of AA using methylene blue-modified  $\text{SiO}_2/\text{ZrO}_2/\text{phosphate}$  CCE electrodes [43]. The results obtained here clearly indicated that DA could be measured without any interference from the presence of a large excess of AA.

### 3.2.6. Simultaneous determination of DA and AA using the SGN/NiPc electrode

Fig. 7 shows the DPV measurements recorded using the SGN/NiPc electrode for simultaneous determination of different concentrations of AA and DA in  $0.5 \text{ mol dm}^{-3}$  KCl solution (pH 5.0). Two well-distinguished anodic peaks, at 0.30 and 0.56 V, corresponded to the oxidation of AA and DA, respectively. The anodic peaks increased in line with the analytes concentrations.

The calibration curves for AA and DA are shown in the inset of Fig. 7. For AA, there was a linear relationship between the peak current and concentrations in the range  $9.00 \times 10^{-5}$  to  $2.11 \times 10^{-3} \text{ mol dm}^{-3}$ , described by the linear regression equation:  $\Delta I_{pa} (\mu\text{A}) = 53.02 (\pm 0.54) [\text{AA}] (\text{mmol dm}^{-3}) + 1.97$

**Table 2**  
Analytical parameters for simultaneous detection AA and DA at several modified electrodes.

Electrode	Method	Linear range ( $\mu\text{mol dm}^{-3}$ )		Sensitivity ( $\mu\text{A mmol dm}^{-3}$ )		Detection limit ( $\mu\text{mol dm}^{-3}$ )		References
		AA	DA	AA	DA	AA	DA	
(AuNPs@PANI/CS/GCE) <sup>a</sup>	DPV	20.0–1600.0	10.0–1700.0	–	–	8.0	5.0	[44]
AuNPs/(ATP-ABA) <sup>b</sup> /GCE	DPV	20.0–140.0	15.0–135.0	68.90	40.70	8.2	9.2	[45]
PEDOT <sup>c</sup> /GCE	SWV <sup>d</sup>	300.0–1500.0	100.0–500.0	12.00	22.00	–	–	[46]
Poly(caffeic acid)/GCE	CV <sup>e</sup>	20.0–1200.0	1.0–40.0	10.70	395.10	9.00	0.40	[47]
SGN/NiPc	DPV	90.0–2110.0	40.0–1080.0	53.02	104.17	0.45	0.26	This work

<sup>a</sup> (Gold nanoparticles@polyaniline/chitosan/glassy carbon electrode).

<sup>b</sup> (4-Aminothiopheno-4-aminobenzoic acid).

<sup>c</sup> Poly(3,4-ethylenedioxy)thiophene.

<sup>d</sup> Square wave voltammetry.

<sup>e</sup> Cyclic voltammetry.

**Table 3**  
Determination of AA and DA in samples made in physiological solution.

No.	DA content ( $10^{-5}$ mol dm <sup>-3</sup> )	AA content ( $10^{-3}$ mol dm <sup>-3</sup> )	DA concentration found ( $10^{-5}$ mol dm <sup>-3</sup> )	Recovery (%)	AA concentration found ( $10^{-3}$ mol dm <sup>-3</sup> )	Recovery (%)
1	8.00	0.80	8.60	107.50	0.87	108.75
2	8.00	0.80	8.66	108.25	0.81	101.25
3	8.00	0.80	8.58	107.25	0.82	102.50
4	8.00	0.80	8.65	108.13	0.88	102.50
Average			8.62		0.85	
Standard derivation			3.86%		3.51%	

( $\pm 0.67$ ),  $r = 0.9994$ . The limit of detection calculated for AA was  $0.45 \mu\text{mol dm}^{-3}$ . Similarly, the peak current of DA showed a linear relationship with concentrations in the range  $4.00 \times 10^{-5}$  to  $1.08 \times 10^{-3}$  mol dm<sup>-3</sup>. The following linear regression equation was obtained:  $\Delta I_{pa} (\mu\text{A}) = 104.17 (\pm 1.33) [\text{DA}] (\text{mmol dm}^{-3}) + 2.50 (\pm 0.85)$ ,  $r = 0.999$ , and the limit of detection was  $0.26 \mu\text{mol dm}^{-3}$ .

In Table 2 is presented a comparison of the analytical parameters of the SGN/NiPc electrode with other modified electrodes reported in the literature for simultaneous determination of AA and DA by electrochemical process [44–47]. The proposed modified electrode presented a lowest limit of detection, revealing itself as a competitive electrode for this analysis, when compared to other modified electrodes.

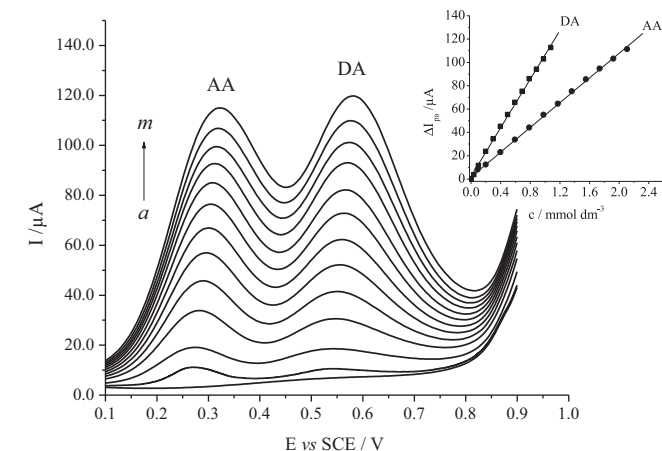


**Fig. 7.** Differential pulse voltammograms recorded for different concentrations of AA and DA, using the SGN/NiPc electrode in  $0.5 \text{ mol dm}^{-3}$  KCl solution (pH 5.0). DA concentrations (from a to m):  $4.00 \times 10^{-5}$ ,  $1.00 \times 10^{-4}$ ,  $2.00 \times 10^{-4}$ ,  $2.98 \times 10^{-4}$ ,  $3.97 \times 10^{-4}$ ,  $4.95 \times 10^{-4}$ ,  $5.93 \times 10^{-4}$ ,  $6.90 \times 10^{-4}$ ,  $7.87 \times 10^{-4}$ ,  $8.84 \times 10^{-4}$ ,  $9.80 \times 10^{-4}$ ,  $1.08 \times 10^{-3}$  mol dm<sup>-3</sup>. AA concentrations (from a to m):  $9.00 \times 10^{-5}$ ,  $2.00 \times 10^{-4}$ ,  $3.97 \times 10^{-4}$ ,  $5.93 \times 10^{-4}$ ,  $7.87 \times 10^{-4}$ ,  $9.80 \times 10^{-4}$ ,  $1.17 \times 10^{-3}$ ,  $1.36 \times 10^{-3}$ ,  $1.55 \times 10^{-3}$ ,  $1.74 \times 10^{-3}$ ,  $1.92 \times 10^{-3}$ , and  $2.11 \times 10^{-3}$  mol dm<sup>-3</sup>. The inset shows the calibration curves for AA and DA.

The analytical performance of the SGN/NiPc electrode was illustrated by the simultaneous quantitative determination of AA and DA in samples. For this purpose, we prepared a series of four test solutions of known concentration consisting of the mixture of DA ( $1.75 \text{ mmol dm}^{-3}$ ) and AA ( $17.47 \text{ mmol dm}^{-3}$ ) prepared in the physiological solution (0.9%, w/v). An aliquot of 1.2 mL of each test solution was pipetted into the electrochemical cell followed by determination of the analytes using the above DPV method. The concentrations of AA and DA were calculated from the calibration graphs and the results are listed in Table 3. The SGN/NiPc electrode showed a good agreement with the analytes added which constitutes in a promising feature for its application in the simultaneous determination of AA and DA in pharmaceutical formulations.

The stability and reproducibility of the SGN/NiPc electrode were investigated by DPV, using a mixture of  $2.11 \times 10^{-3}$  mol dm<sup>-3</sup> AA and  $1.27 \times 10^{-3}$  mol dm<sup>-3</sup> DA. The relative standard deviations (R.S.D.) of the oxidation peak current, using 10 successive determinations, were 3.67% and 3.53% for AA and DA, respectively. A set of four modified electrodes, prepared under identical conditions, gave R.S.D. values of 3.45% and 3.12% for AA and DA, respectively. After 11 months of use, the current response of the modified electrode decreased by about 5%. This long-term stability was achieved by washing and drying the modified electrode after each use. Overall, the results demonstrate that the SGN/NiPc electrodes possessed good characteristics in terms of stability and reproducibility.

#### 4. Conclusions

The sol-gel procedure, performed using two steps with different catalysts, was employed to manufacture three types of carbon ceramic material (SGN, SGF, and SGNF) possessing different porosities and specific surface areas. The preparation procedures resulted in different morphologies of the materials, and phase segregation of C particles was only observed for SGN, improving its conductivity compared to the other two materials. XPS measurements revealed a greater Ni/Si atomic ratio for SGN/NiPc, after *in situ* immobilization of Ni(II) phthalocyanine on the surface of the carbon ceramic matrices.

The NiPc-modified matrices showed catalytic activity during the oxidation of dopamine. The SGN/NiPc electrode provided greater sensitivity than the other two modified electrodes, due to a greater prevalence of electroactive species and good conductivity. Well-defined and well-separated voltammetric oxidation peaks were obtained using this electrode, enabling the simultaneous determination of dopamine and ascorbic acid. There was no interference from AA, even in large excess, during the determination of DA using the SGN/NiPc electrode. The modified electrode showed good repeatability in terms of both measurements and electrode preparation, and continued to provide stable, sensitive, selective, and reproducible responses for AA and DA after several months of usage. This robust electrode therefore has considerable potential for the simultaneous determination of DA and AA in commercial and environmental applications.

### Acknowledgments

YG and AAT are indebted to FAPESP and CNPq for financial support. Doctoral fellowships were provided by CNPq/TWAS (to AR) and CAPES (to SBAB).

### References

- [1] A. Walcarius, *Electroanalysis with pure, chemically modified, and sol-gel derived silica-based materials*, *Electroanalysis* 13 (8–9) (2001) 701.
- [2] A. Walcarius, M.M. Collinson, *Analytical chemistry with silica sol-gels: traditional routes to new materials for chemical analysis*, *Annual Review of Analytical Chemistry* 2 (2009) 121.
- [3] L. Rabinovich, O. Lev, *Sol-gel derived composite ceramic carbon electrodes*, *Electroanalysis* 13 (4) (2001) 265.
- [4] L.T. Arenas, P.C.M. Villis, J. Arguello, R. Landers, E.V. Benvenuti, Y. Gushikem, Niobium oxide dispersed on a carbon-ceramic matrix,  $\text{SiO}_2/\text{C}/\text{Nb}_2\text{O}_5$ , used as an electrochemical ascorbic acid sensor, *Talanta* 83 (2010) 241.
- [5] I. Svancara, K. Vytras, K. Kalcher, A. Walcarius, J. Wang, *Carbon paste electrodes in facts, numbers, and notes: a review on the occasion of the 50-years jubilee of carbon paste in electrochemistry and electroanalysis*, *Electroanalysis* 21 (2009) 7.
- [6] E. Marafon, L.T. Kubota, Y. Gushikem, FAD-modified  $\text{SiO}_2/\text{ZrO}_2/\text{C}$  ceramic electrode for electrocatalytic reduction of bromate and iodate, *Journal of Solid State Electrochemistry* 13 (2009) 377.
- [7] V. Loryuenyong, T. Muanghom, T. Apinyanukul, P. Rutthongjan, *Synthesis of templated mesoporous silica nanoparticles under base catalysis*, *Advances in Applied Ceramics* 110 (2011) 335.
- [8] L. Li, B. Yalcin, B.N. Nguyen, M.A.B. Meador, M. Cakmak, *Flexible nanofiber-reinforced aerogel (xerogel) synthesis, manufacture, and characterization*, *Applied Materials and Interfaces* 11 (2009) 2491.
- [9] U. Salan, A. Altindal, A.R. Ozkaya, B. Salih, O. Bekaroglu, *Photovoltaic and electrocatalytic properties of novel ball-type phthalocyanines bridged with four dicumarol*, *Dalton Transactions* 41 (2012) 5177.
- [10] C.G. Bezzu, M. Helliwell, B.M. Kariuki, N.B. McKeown, *Synthesis and crystal structure of a novel phthalocyanine-calixarene conjugate*, *Porphyryns Phthalocyanines Journal* 15 (2011) 686.
- [11] T. Nyonkong, *Effects of substituents on the photochemical and photophysical properties of main group metal phthalocyanines*, *Coordination Chemistry Reviews* 251 (2007) 1707.
- [12] J.H. Zagal, S. Griveau, J.F. Silva, T. Nyokong, F. Bedioui, *Metallophthalocyanine-based molecular materials as catalysts for electrochemical reactions*, *Coordination Chemistry Reviews* 254 (2010) 2755.
- [13] L.S.S. Santos, R. Landers, Y. Gushikem, *Application of manganese(II) phthalocyanine synthesized in situ in the  $\text{SiO}_2/\text{SnO}_2$  mixed oxide matrix for determination of dissolved oxygen by electrochemical techniques*, *Talanta* 85 (2011) 1213.
- [14] D. Zheng, X. Liu, D. Zhou, S. Hu, *Sensing of nitric oxide using a glassy carbon electrode modified with an electrocatalytic film composed of dihexadecyl hydrogen phosphate, platinum nanoparticles, and acetylene black*, *Microchimica Acta* 176 (2012) 49.
- [15] A.P. Gutierrez, S. Griveau, C. Richard, A. Pailletet, S.G. Granados, F. Bedioui, *Hybrid materials from carbon nanotubes, nickel tetrasulfonated phthalocyanine and thin polymer layers for the selective electrochemical activation of nitric oxide in solution*, *Electroanalysis* 21 (2009) 2303.
- [16] E.F. Perez, L.T. Kubota, A.A. Tanaka, G. Oliveira Neto, *Anodic oxidation of cysteine catalysed by nickel tetrasulfonated phthalocyanine immobilized on silica gel modified with titanium (IV) oxide*, *Electrochimica Acta* 43 (12–13) (1998) 1665.
- [17] Z.H. Wen, T.F. Kang, *Determination of nitrite using sensors based on nickel phthalocyanine polymer modified electrodes*, *Talanta* 62 (2) (2004) 351.
- [18] T.C. Canevari, R.C.S. Luz, Y. Gushikem, *Electrocatalytic determination of nitrite on a rigid disk electrode having cobalt phthalocyanine prepared in situ*, *Electroanalysis* 20 (7) (2008) 765.
- [19] J. Arguello, H.A. Magosso, R.R. Ramos, T.C. Canevari, R. Landers, V.L. Pimentel, Y. Gushikem, *Structural and electrochemical characterization of a cobalt phthalocyanine bulk-modified  $\text{SiO}_2/\text{SnO}_2$  carbon ceramic electrode*, *Electrochimica Acta* 54 (2009) 1948.
- [20] A. Rahim, S.B.A. Barros, L.T. Arenas, Y. Gushikem, *In situ immobilization of cobalt phthalocyanine on the mesoporous carbon ceramic  $\text{SiO}_2/\text{C}$  prepared by the sol-gel process. Evaluation as an electrochemical sensor for oxalic acid*, *Electrochimica Acta* 56 (2011) 1256.
- [21] K. Wang, J.-J. Xu, K.-S. Tang, H.-Y. Chen, *Solid-contact potentiometric sensor for ascorbic acid based on cobalt phthalocyanine nanoparticles as ionophore*, *Talanta* 67 (2005) 798.
- [22] A. Rahim, S.B.A. Barros, L.T. Kubota, Y. Gushikem,  *$\text{SiO}_2/\text{C}/\text{Cu(II)}$ phthalocyanine as a biomimetic catalyst for dopamine monoxygenase in the development of an amperometric sensor*, *Electrochimica Acta* 56 (2011) 10116.
- [23] T. Łuczak, *Preparation and characterization of the dopamine film electrochemically deposited on a gold template and its applications for dopamine sensing in aqueous solution*, *Electrochimica Acta* 53 (2008) 5725.
- [24] X.Q. Lin, L. Zhang, *Simultaneous determination of dopamine and ascorbic acid at glutamic acid modified graphite electrode*, *Analytical Letters* 34 (2001) 1585.
- [25] A. Salimi, H. Mamkhezri, R. Hallaj, *Simultaneous determination of ascorbic acid, uric acid and neurotransmitters with a carbon ceramic electrode prepared by sol-gel technique*, *Talanta* 70 (2006) 823.
- [26] B. Habibi, M.H. Pournaghi-Azar, *Simultaneous determination of ascorbic acid, dopamine and uric acid by use of a MWCNT modified carbon-ceramic electrode and differential pulse voltammetry*, *Electrochimica Acta* 55 (2010) 5492.
- [27] K.-H. Xue, F.-F. Tao, W. Xu, S.-Y. Yin, J.-M. Liu, *Selective determination of dopamine in the presence of ascorbic acid at the carbon atom wire modified electrode*, *Journal of Electroanalytical Chemistry* 578 (2005) 323.
- [28] M. Toledo, A.M.S. Lucho, Y. Gushikem, *In situ preparation of Co phthalocyanine on a porous silica gel surface and the study of the electrochemical oxidation of oxalic acid*, *Journal of Materials Science* 39 (2004) 6851.
- [29] S. Brunauer, P.H. Emmett, E. Teller, *Adsorption of gases in multimolecular layers*, *Journal of the American Chemical Society* 60 (1938) 309.
- [30] E.P. Barrett, L.G. Joyner, P.P. Halenda, *The determination of pore volume and area distributions in porous substances. I. computations from nitrogen isotherms*, *Journal of the American Chemical Society* 73 (1951) 373.
- [31] E.M. Giroto, I.A. Santos, *Medidas de resistividade elétrica DC em sólidos: como efetua-las corretamente*, *Química Nova* 25 (2002) 639.
- [32] S.J. Gregg, K.S.W. Sing, *Adsorption Surface Area and Porosity*, 2nd ed., Academic Press, London, 1982.
- [33] K.S.W. Sing, D.H. Everett, R.A.W. Haul, L. Moscou, R.A. Pierotti, J. Rouquerol, T. Siemieniowska, *Reporting physisorption data for gas/solid systems with special reference to the determination of surface area and porosity*, *Pure and Applied Chemistry* 57 (1985) 603.
- [34] T.N.M. Bernards, M.J. Bommel, J.A.J. Jansen, *The effect of HF in a two-step sol-gel process of TEOS*, *Journal of Sol-Gel Science and Technology* 13 (1998) 749.
- [35] S. Ray, S. Vasudevan, *Encapsulation of cobalt phthalocyanine in zeolite-y: evidence for nonplanar geometry*, *Inorganic Chemistry* 42 (2003) 1711.
- [36] J. Ahlund, K. Nilson, J. Kjeldgaard, S. Berner, N. Martensson, C. Puglia, B. Brena, M. Nyberg, Y. Luo, *The electronic structure of iron phthalocyanine probed by photoelectron and x-ray absorption spectroscopies and density functional theory calculations*, *Journal of Chemical Physics* 125 (2006) 034709.
- [37] S.F. Moya, R.L. Martins, M. Schmal, *Monodispersed and nanostructured Ni/SiO<sub>2</sub> catalyst and its activity for non oxidative methane activation*, *Applied Catalysis A* 396 (2011) 159.
- [38] T.L. Barr, *An ESCA study of the termination of the passivation of elemental metals*, *Journal of Physical Chemistry* 82 (1978) 1801.
- [39] IUPAC, *Recommendations for the definition, estimation and use of the detection limit*, *Analyst* 112 (1987) 199.
- [40] M. Etienne, A. Quach, D. Grosso, L. Nicole, C. Sanchez, A. Walcarius, *Molecular transport into mesostructured silica thin films: electrochemical monitoring and comparison between p6m, P6 3//WWIC, and Pm3n structures*, *Chemistry of Materials* 19 (2007) 844.
- [41] M. Mazloum-Ardakani, Z. Taleat, *Investigation of electrochemistry behavior of hydroxylamine at glassy carbon electrode by indigocarmine*, *International Journal of Electrochemical Science* 4 (2009) 694.
- [42] N. Nasirizadeh, H.R. Zare, *Differential pulse voltammetric simultaneous determination of noradrenalin and acetaminophen using a hematoxylin biosensor*, *Talanta* 80 (2009) 656.
- [43] J. Arguello, V.L. Leidens, H.A. Magosso, R.R. Ramos, Y. Gushikem, *Simultaneous voltammetric determination of ascorbic acid, dopamine and uric acid by methylene blue adsorbed on a phosphorylated zirconia-silica composite electrode*, *Electrochimica Acta* 54 (2008) 560.
- [44] L. Yang, S. Liu, Q. Zhang, F. Li, *Simultaneous electrochemical determination of dopamine and ascorbic acid using AuNPs@polyaniline core-shell nanocomposites modified electrode*, *Talanta* 89 (2012) 136.
- [45] L. Zhang, X. Jiang, *Attachment of gold nanoparticles to glassy carbon electrode and its application for the voltammetric resolution of ascorbic acid and dopamine*, *Journal of Electroanalytical Chemistry* 583 (2005) 292.
- [46] V.S. Vasantha, S.-M. Chen, *Electrocatalysis and simultaneous detection of dopamine and ascorbic acid using poly(3,4-ethylenedioxy)thiophene film modified electrodes*, *Journal of Electroanalytical Chemistry* 592 (2006) 77.
- [47] N.B. Li, W. Ren, Q. Luo, *Simultaneous voltammetric measurement of ascorbic acid and dopamine on poly(caffeic acid)-modified glassy carbon electrode*, *Journal of Solid State Electrochemistry* 12 (2008) 693.